

Fabrication of a Superhydrophobic sponge surface Coating by Fe₂O₃-MgO nanocomposite

sabah H. Jumaah¹ Raad S. Sabry² Wisam J. Aziz³

^{1,2,3} Physics Department, College of Science, Mustansiriyah University, Baghdad 10052, Iraq :

shjedu@uomustansiriyah.edu.iq¹ , drraad_sci@uomustansiriyah.edu.iq² ,

wisamj.aziz@uomustansiriyah.edu.iq³

ABSTRACT

In this study, Fe₂O₃ (NPs), MgO(NPs) and Fe₂O₃-MgO nanocomposite were successfully synthesized by hydrothermal method. By adding different molar ratios of stearic acid (0.05, 0.2 mol) using dip coating method to the fabrication of superhydrophobic Fe₂O₃-MgO nanocomposite coated on sponge surface was successfully manufactured. The stearic acid acts to reduce the surface free energy. The XRD pattern of Fe₂O₃-MgO nanocomposite shows that the XRD pattern consists of diffraction peaks of both iron oxide and magnesium oxide. FESEM images of coated sponges show that all coated sponges share a strikingly similar morphology. They show a layered structure and roughness in the surface topography, with plates arranged parallel to each other. According to the AFM results, the nanocomposite (Fe₂O₃-MgO) showed the highest surface roughness among the three samples, with Ra reaching 69 nm and Rq 83.30 nm. The contact angles for samples with (0.05 and 0.2) are equal to 153.8°, 15° respectively. Therefore, there is a direct relationship between the molar ratio of fatty acid nanocomposite and the contact angle. As the molar ratio increases, the contact angle also increases, due to the increased surface roughness.

Keywords: Fe₂O₃-MgO nanocomposite, stearic acid, sponge surface, hydrothermal method, super hydrophobicity

1. Introduction

Surface engineering has witnessed remarkable advancements in recent years, introducing innovative materials and coatings with transformative properties. Among these, superhydrophobic coatings have emerged as a remarkable avenue, offering surfaces with unprecedented water-repellent characteristics. Inspired by nature's marvels, superhydrophobic surfaces have found applications across industries, from self-cleaning mechanisms to anti-corrosion solutions. A significant stride in this direction is the development of Fe₂O₃-MgO superhydrophobic coatings on sponge surfaces, a promising approach that combines the advantages of nanoparticles and surface chemistry to achieve exceptional hydrophobicity and multifaceted applications [1,3]. The development of advanced materials and surface coatings

^{*}Corresponding author : sabah H. Jumaah¹

E-mail: shjedu@uomustansiriyah.edu.iq

has revolutionized various industries, ranging from aerospace to healthcare. Among these innovations, superhydrophobic coatings have garnered significant attention due to their remarkable water-repellent properties and potential applications in numerous fields. The combination of unique properties offered by superhydrophobic surfaces, such as self-cleaning, anti-corrosion, and anti-icing, has led to their exploration in various practical scenarios. One such promising advancement is the Fe₂O₃-MgO superhydrophobic coating on sponge surfaces, which has shown immense potential for enhancing material performance and expanding the scope of superhydrophobic applications [1-4]. Superhydrophobic surfaces, inspired by nature's lotus leaves and water strider insects, exhibit an extraordinary ability to repel water and resist wetting. These surfaces are characterized by their high-water contact angles (typically greater than 150 degrees) and low contact angle hysteresis. The superhydrophobic effect arises from the synergy of microscale and nanoscale surface features, combined with low surface energy materials. Such a combination creates a dual-scale roughness, preventing water from fully wetting the surface and causing it to bead up and roll off easily [4]. The integration of iron oxide (Fe₂O₃) and magnesium oxide (MgO) nanoparticles into superhydrophobic coatings has recently emerged as an intriguing avenue for enhancing the performance of superhydrophobic surfaces. The combination of these nanoparticles imparts both hydrophobicity and durability to the coated substrate. Iron oxide nanoparticles offer enhanced mechanical stability, and their chemical properties provide an excellent foundation for adhesion of the hydrophobic molecules. On the other hand, magnesium oxide nanoparticles contribute

to the low surface energy required for superhydrophobicity [2]. The integration of iron oxide (Fe₂O₃) and magnesium oxide (MgO) nanoparticles within superhydrophobic coatings has unlocked new dimensions for surface engineering. Iron oxide nanoparticles contribute mechanical stability, and their chemistry forms a robust substrate for hydrophobic moieties. Simultaneously, magnesium oxide nanoparticles introduce the low surface energy required for the superhydrophobic effect. This combination synergistically enhances the coating's water-repellent characteristics and durability [2]. Synthesizing Fe₂O₃-MgO superhydrophobic coatings involves a strategic process. First, sponge surfaces are prepared, creating a suitable substrate. Next, a carefully designed deposition method, such as sol-gel or spray coating, is employed to embed the Fe₂O₃ and MgO nanoparticles onto the sponge surface. The nanoparticles introduce controlled roughness at micro and nanoscales, while hydrophobic agents like perfluorinated compounds are applied to further reduce the surface energy and maximize hydrophobicity [2]. The synthesis of Fe₂O₃-MgO superhydrophobic coatings involves a multi-step process. Initially, sponge surfaces are prepared to ensure a suitable substrate. Next, a combination of Fe₂O₃ and MgO nanoparticles is deposited onto the sponge surface through methods like sol-gel or spray coating. The nanoparticles create a rough surface morphology at both micro and nanoscales, promoting the desired superhydrophobic effect. Finally, hydrophobic agents such as perfluorinated compounds are applied to further reduce the surface energy, maximizing the water-repellent properties [5]. The Fe₂O₃-MgO superhydrophobic coating on sponge surfaces holds immense promise for a wide range of applications across industries. The sponge's inherent porosity, combined with the superhydrophobic characteristics, creates a versatile platform for various applications [2]. The sponge coated with Fe₂O₃-MgO superhydrophobic layers can be used to efficiently separate oil and water mixtures, finding application in environmental cleanup and industrial processes. By repelling water, the coated sponge surfaces can be used to enhance insulation properties, preventing moisture penetration in applications like construction and electronics [6]. The superhydrophobic coating's ability to repel water helps protect metallic surfaces from corrosion and degradation, prolonging the lifespan of structures and equipment [7]. The coating's self-cleaning properties are advantageous for medical devices and implants, reducing the risk of

biofilm formation [8-9]. Hydrophobic surfaces were successfully created using Fe₂O₃-MgO nanocomposite and by dipping on the sponge surface. For this purpose, the Fe₂O₃-MgO nanocomposite was first synthesized and characterized, and the subsequent coverage on the sponge surface, contact angle and morphology of the composite surfaces were studied. The effect of changing the molar ratio of fatty acid to Fe₂O₃-MgO nanocomposite was also studied and analyzed.

2. Experimental

a. Fabrication of the α -Fe₂O₃ nanoparticles powder by hydrothermal method.

2g of (FeCl₃) were dissolved in distilled water (100ml) under stirring for 30 min to complete dissolution at room temperature. Subsequently (15ml) of ammonia (ratio 1:1, H₂O:NH₃) was added to solution and stirred to another (30 min.).the final solution was put inside autoclave and sealed tightly then placed in the furnace at 120 °C for 5 h. Afterward, a blackish-brown powder is obtained after which it is washed with distilled water several times under centrifugation. Then annealing at 150°C for 4h.

b. Fabrication of MgO nanoparticles powder by hydrothermal method.

(1.02g) of mg(NO₃)₂.6H₂O and (0.56) of HMT were dissolved in (80ml) of D.W. and stirred for (30 min.) to complete dissolution. The solution transfer to autoclave and sealed tightly before being placed in the furnace at 100 °C for 3 hours. Finally, the white precipitate was collected by centrifugation, repeatedly washed with DW and ethanol several times, and annealing at 400 °C for 3 hours.

c. Preparation of Fe₂O₃-MgO nanocomposite

0.15 g of synthesized iron oxide was mixed with 80 ml of water and stirred for 30 min at ambient temperature. Then NaOH was added to it with a molar ratio of 1:1 until the pH reached 10 and it was kept under stirring for 30 min. In the next step, 1.4 g of magnesium nitrate was added to the solution. After stirring for 30 min, the final solution was transferred to the autoclave and placed in the oven at 120 °C for 2 h. The resulting powder was separated by centrifugation and washed several times with deionized water and ethanol. Finally, it was calcined in the furnace at 400 °C.

d. preparation of Fe₂O₃-MgO nanocomposite superhydrophobic sponge by dip coting method.

For superhydrophobic surfaces, the doped Fe₂O₃-MgO nanocomposite is prepared by the precipitation method. In a typical modification, 30 mg of dry powders of Fe₂O₃-MgO doped with different molar ratios of stearic acid (0.01M, 0.05M, 0.1M, and 0.2M) were dispersed in a 20 mL ethanol solution with stirring for 60 min at a temperature of 70 °C. The sponge as substrate was dip coating in the final solution for and dried in the oven at a temperature 50 °C for 30 min.

3. Results and discussion

3.1. XRD Analysis

The X-ray diffraction (XRD) pattern of Fe₂O₃ nanoparticles is shown in figure (1-a). In the case of Fe₂O₃ nanoparticles, the analysis is guided by the standard reference XRD pattern for α -Fe₂O₃, which is documented as JCPDS Card No. 01-086-0550. The XRD pattern of these nanoparticles reveals several peaks. These peaks indicate the presence of a crystalline phase. The most intense

peak is found at a 2θ angle of 33.28° , which corresponds to the (104) plane of the iron oxide crystal structure. Additional peaks are observed at 2θ angles of 24.27° , 35.78° , 40.99° , 49.60° , 54.19° , 57.68° , 62.56° , 64.149° , 72.06° , and 75.63° . These correspond to the (012), (110), (113), (024), (116), (018), (214), (300), (1010), and (220) planes of the iron oxide crystal structure respectively [10].

Figure (1-b) presents the XRD pattern for nanoparticles of magnesium oxide. The pattern reveals the presence of a crystalline phase within the nanoparticles, as indicated by several peaks. The most pronounced peak is observed at a 2θ angle of 42.70° , which aligns with the (200) plane of the magnesium oxide's crystal structure. Other peaks are found at 2θ angles of 36.64° , 62.00° , 74.29° , and 78.28° , corresponding to the (111), (220), (311), and (222) planes of the magnesium oxide crystal structure respectively. The observed diffraction peaks closely match the standard cubic phase of Magnesium Oxide, as documented in JCPDS card No. 01-087-0653 [11]. The XRD analysis is a powerful tool not only for determining the crystal structure and orientation of materials, but also for estimating the size of the crystallites, which are the individual crystals that constitute a material. The Debye-Scherrer formula is a widely accepted method for deriving the crystallite size from XRD data. This formula establishes a relationship between the crystallite size and the X-ray wavelength, line broadening, and Bragg angle of the diffraction peak. Here is the Debye-Scherrer formula used for calculating the crystallite size:

$$D = \frac{k\lambda}{\beta \cos \theta} \quad (1)$$

In this formula, D represents the crystallite size, k stands for the shape factor, λ is the X-ray wavelength, β denotes the line broadening at half maximum intensity (FWHM), in radians and θ symbolizes the Bragg angle. The shape factor (k) accounts for the shape of the crystallites and its value is determined by the crystal structure of the material. The crystallite size was determined to be 42 nm for the (104) plane of the Fe_2O_3 nanoparticles and approximately 9 nm for the (200) plane of the MgO nanoparticles. The XRD parameters including Bragg angles, miller indices, β , d-spacing and relative intensity for Fe_2O_3 and MgO nanoparticles are listed. The XRD pattern for the Fe_2O_3 -MgO nanocomposite, as shown in Figure (1-c), exhibits several peaks. In the study of the Fe_2O_3 -MgO nanocomposite, it's important to note that the XRD pattern aligns well with both reference codes for iron oxide and magnesium oxide: 01-086-0550 for iron oxide and 01-087-0653 for magnesium oxide. This consistency validates the presence of both iron and magnesium oxide phases in the nanocomposite. The most intense peak is observed at a 2θ angle of 33.3075° , which corresponds to the (104) plane of the iron oxide crystal structure. Additional peaks related to the iron oxide phase are seen at 2θ angles of 24.30° , 35.79° , 41.01° , 49.62° , 54.22° , 57.72° , 62.48° , 64.19° , 72.13° , and 75.55° . These correspond to the (012), (110), (113), (024), (116), (018), (214), (300), (1010) and (220) planes of the iron oxide crystal structure respectively. Peaks related to the magnesium oxide phase are detected at a 2θ angle of 43.01° corresponding to the (200) plane of the magnesium oxide crystal structure, and at a 2θ angle of 78.67° corresponding to the (222) plane of the magnesium oxide crystal structure .

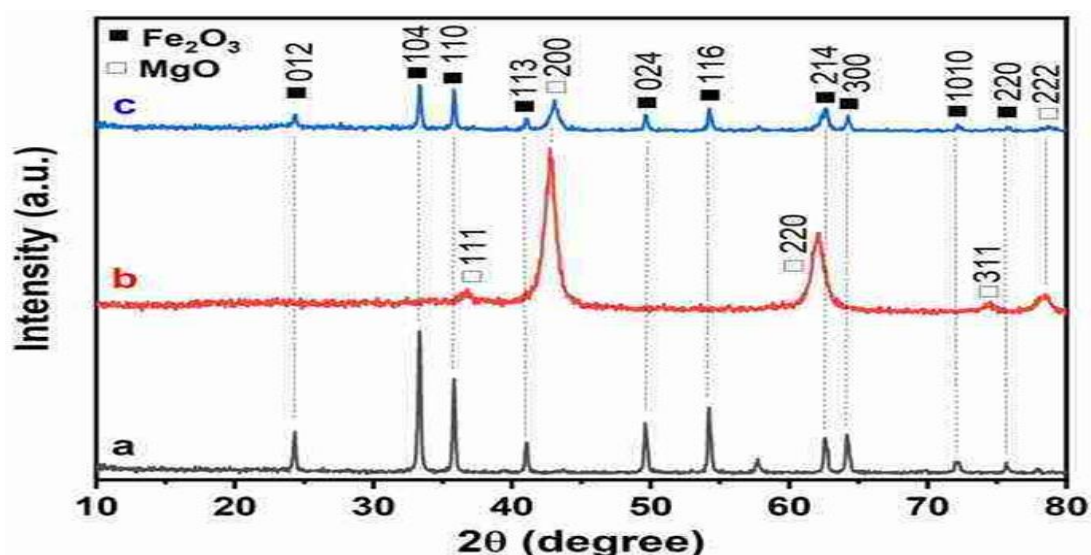


Fig. 1. The XRD patterns of (a) α -Fe₂O₃ NPs, (b) MgO NPs and (c) Fe₂O₃-MgO nanocomposite

3-2 Surface morphology

The surface morphology of the coated sponge was investigated by FESEM studies. Figure 2 provides a detailed view of the FESEM images of the coated sponge. Upon closer inspection, it becomes clear that all painted sponges share a strikingly similar shape. They exhibit a multilayer structure and agglomerate to form a rough surface structure, and both high roughness and low surface energy are key factors necessary to achieve a highly superhydrophobic surface, with plates arranged parallel to each other. This arrangement ensures that the entire surface of the sponge is completely covered. Nanocomposite sheets contribute significantly to this coverage. They are stacked almost uniformly on top of each other, creating a dense, even layer on top of the sponge. This almost uniform stacking is a key factor in promoting the sponge's overall coverage.

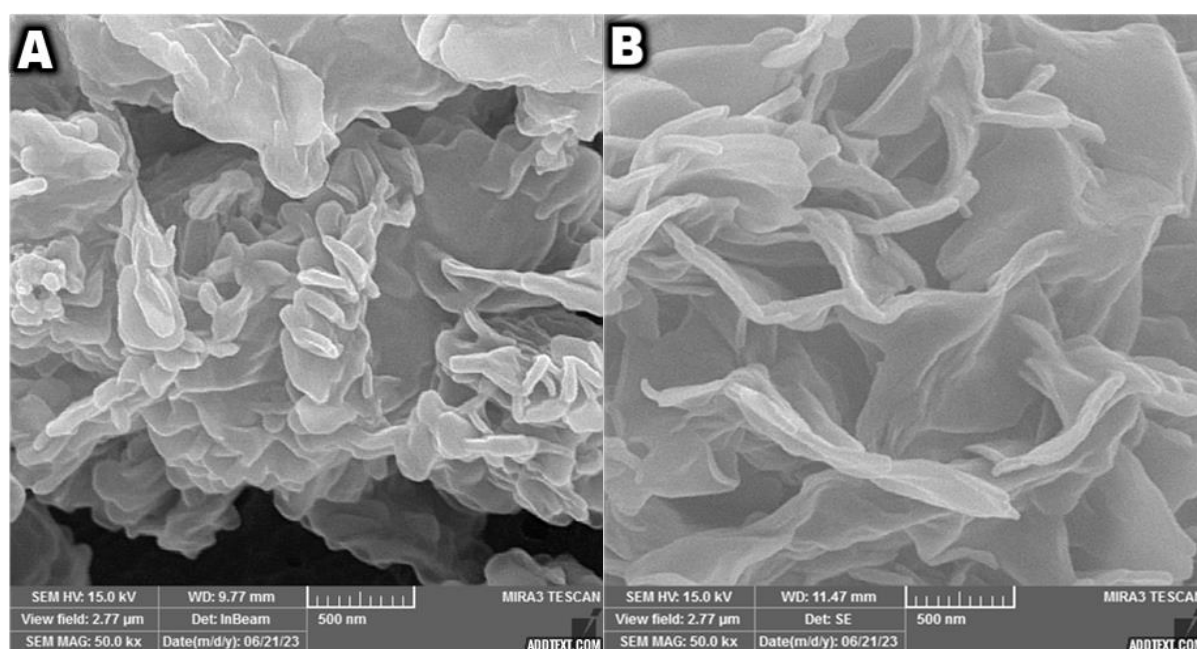


Fig. 2. The FESEM images of coated sponges with different x values (a) x=0.05, (b) x=0.2

Figure 3 shows FESEM images of the cross-section of the sponge coated with different molar ratios (0.05,0.2). It is clear from the observations that the iron and magnesium oxide nanocomposites provide comprehensive coverage of the network and pore structure of the sponge. This complete coverage ensures that every nook and cranny of the sponge's surface is coated with nanocomposites. In SEM images, Fe_2O_3 -MgO nanocomposites can be clearly distinguished from the sponge structure based on their color. The nanocomposites appear in a lighter shade, while the spongy structure appears in a darker shade. This contrast in colors highlights not only the full coverage of the nanocomposites, but also the complex network and porous structure of the sponge. This means that a spongy surface with low surface energy and high roughness was achieved. The main factor of surface superhydrophobic depends on the combination of the surface roughness, 153° , and 158.8° contact angles of the surface-modified samples performed for Fe_2O_3 -MgO, all of which possess a high degree of superhydrophobic material. Surface with angular contact More than 150° .

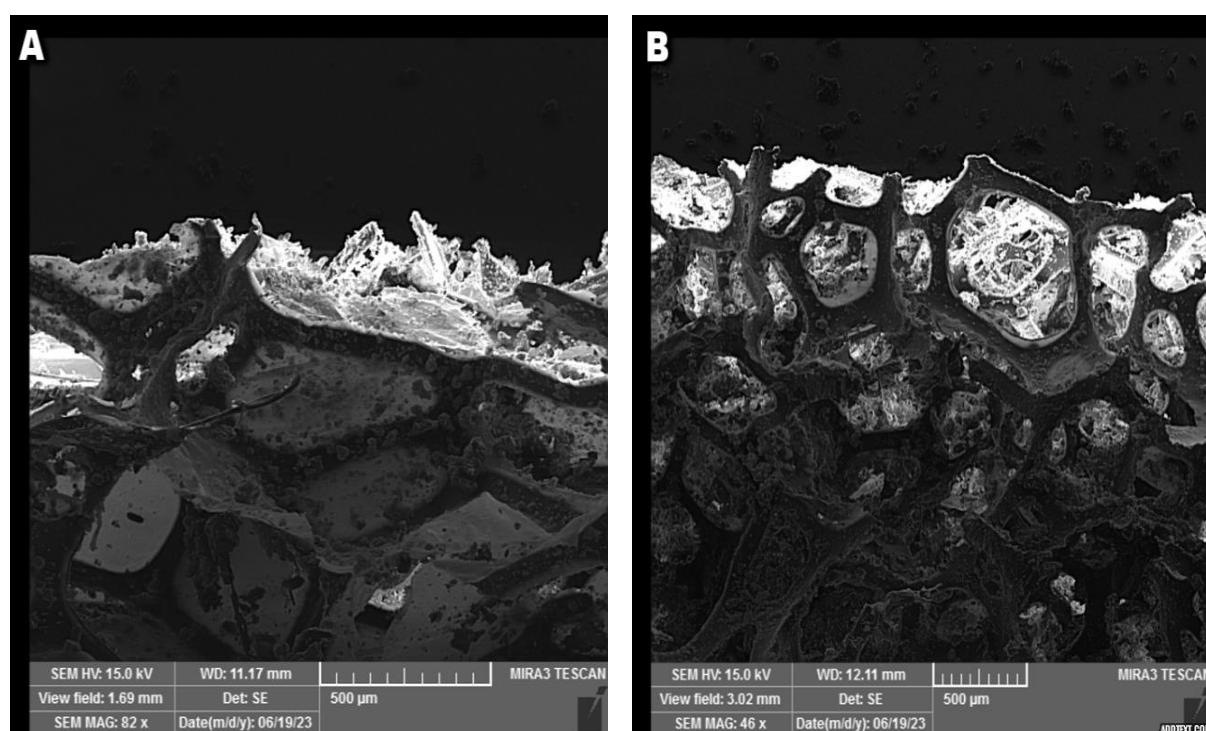


Fig. 3. Cross section of coated sponges with different x values (a) $x=0.05$, (b) $x=0.2$

3.3. AFM

The AFM images of Fe_2O_3 , MgO nanoparticles and Fe_2O_3 -MgO nanocomposite are shown in figure 6. Also, the root mean square of the surface roughness (R_q) and arithmetic roughness average (R_a) of various samples are listed in table 2. The R_q and R_a values for each sample are critical parameters that provide insights into the topographical characteristics of the samples. A higher value indicates a rougher surface, while a lower value suggests a smoother surface. By comparing these values, we can gain a better understanding of the surface properties of each sample. According to table 2 and figure 6, the Fe_2O_3 -MgO nanocomposite exhibited the highest surface roughness among the three samples, with an R_a of 69.41 nm and an R_q of 83.30 nm. This suggests that the composite's surface is the roughest, which could be due to the combination of Fe_2O_3 and MgO nanoparticles. On the other hand, Fe_2O_3 nanoparticles showed the lowest surface roughness, with an R_a of 48.39 nm and an R_q of 59.60 nm. This indicates that among the three samples, Fe_2O_3 nanoparticles have the smoothest surface. The MgO

nanoparticles had an R_a of 63.18 nm and an R_q of 80.25 nm, placing it between the Fe₂O₃ nanoparticles and the Fe₂O₃-MgO nanocomposite in terms of surface roughness.

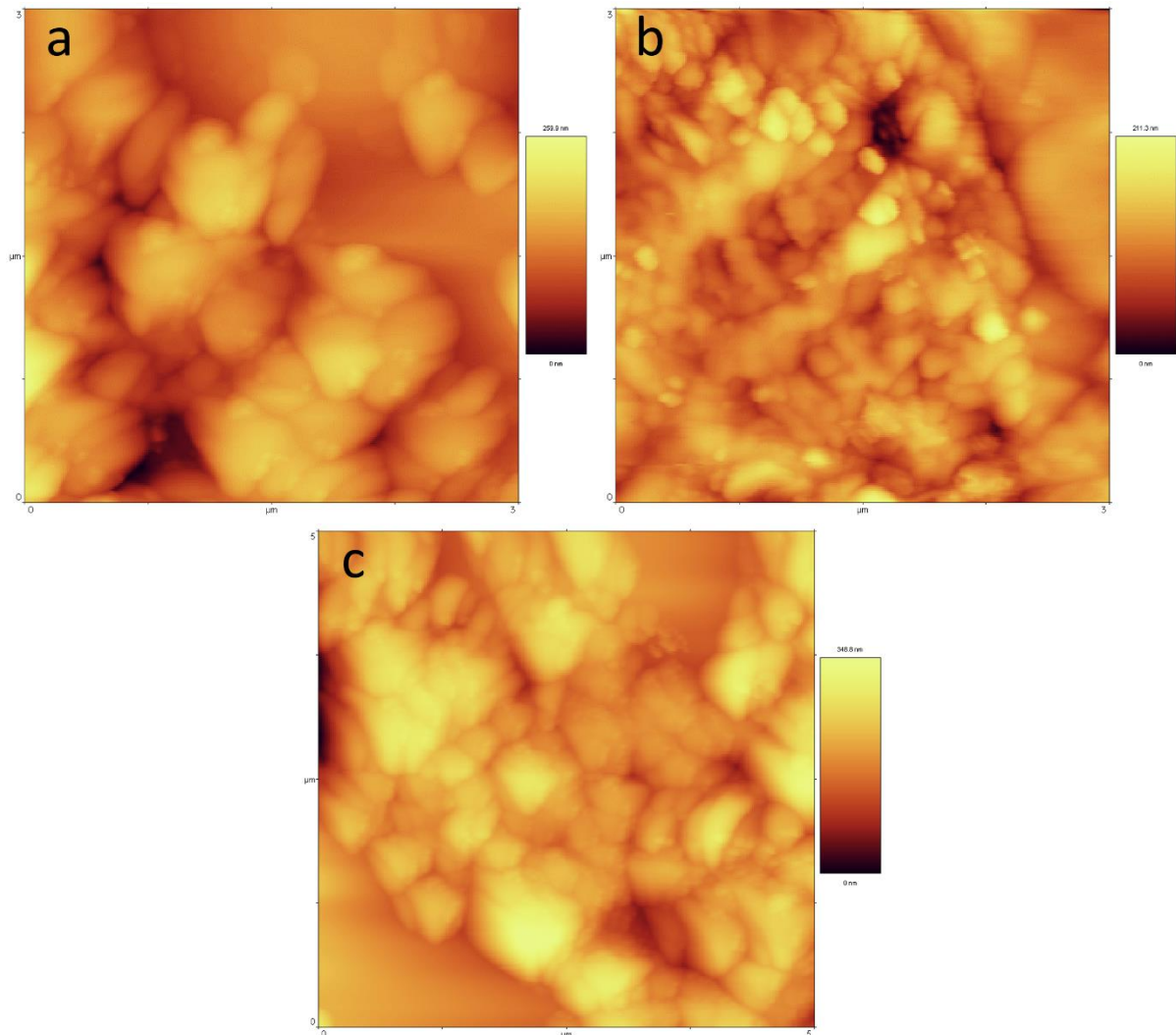


Fig. 4. AFM images of (a) Fe₂O₃, (b) MgO and Fe₂O₃-MgO nanocomposite

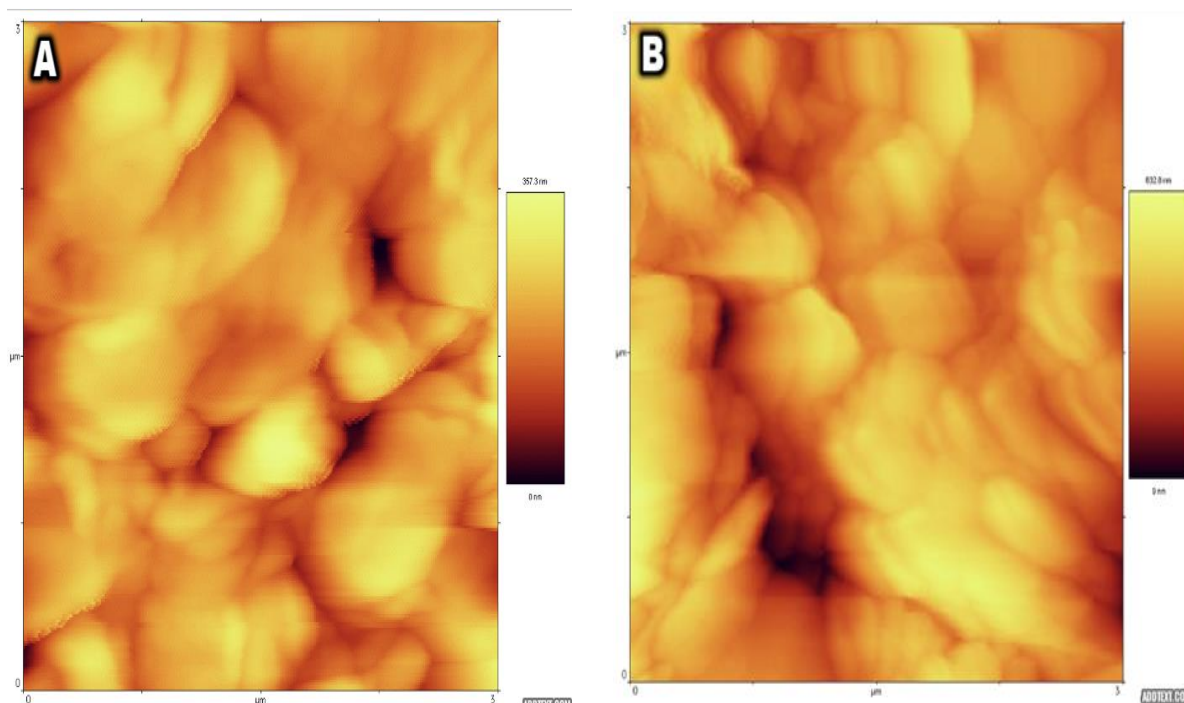
Table 1. The surface roughness of Fe₂O₃, MgO and Fe₂O₃-MgO nanocomposite

Sample	R_a	R_q
Fe ₂ O ₃	48.39	59.60
MgO	63.18	80.25
Fe ₂ O ₃ -MgO	69.41	83.30

Figure 7 shows the AFM images of coated sponges with different values of x . also, the surface roughness of these samples are reported in table 3. Based on the AFM analysis results, it's observed that as the value of x increases, both the R_a and R_q values also increase. This indicates that the surface of the sponge becomes rougher. Specifically, for the sample with $x=0.05$, the R_a and R_q values are the lowest, indicating that this sample has the smoothest surface among all. On the other hand, the sample with $x=0.2$ has the highest R_a and R_q values, suggesting that it has the roughest surface, This roughness helps to form a superhydrophobic surface.

Table 2. The surface roughness of coated sponges with different values of x

Sample	R _a	R _q
X=0.05	100.13	121.75
X=0.2	119.87	161.09

**Fig5.** The AFM images of coated sponges with different x values: (a) x=0.05, (b) x=0.2,

3.4. Contact Angle (CA) measurement

The contact angle is a measure of the wetting behavior of a liquid on a solid surface. It is defined as the angle formed by a liquid at the three-phase boundary where a liquid, gas, and solid intersect. A high contact angle indicates that the liquid does not spread easily on the surface, while a low contact angle means that the liquid wets the surface well. In this study, two sponges were coated with mixtures of stearic acid and iron oxide-magnesium oxide nanocomposite. The molar ratio of stearic acid to nanocomposite in these two mixtures was chosen as, 0.05, and 0.2. The contact angle measurements for these two coated sponges were done. Figure 9 shows the images of the contact angle measurements for the sponges coated with x values of 0.05 and 0.2, respectively. Also, the contact angle values of the sponges coated with different x values are shown in Table 4. According to Table 4 and Figure 9, the contact angles of the samples with x values of 0.05 and 0.2 are respectively 150.9° and 158.8° . Samples with x values of 0.05 show clear hydrophobic properties. It is worth noting that the sample with 0.2 is the most superhydrophobic, since its contact angle is larger than 150° . Comparison of the two samples indicates a direct relationship between the molar ratio of fatty acid to nanocomposite and the contact angle. As the molar ratio increases, the contact angle also increases, as shown in Figure 6. This is due to the increase in surface roughness with increasing fatty acid ratio. The increase in surface roughness with increasing value of x plays an

important role in enhancing the hydrophobicity of the surface. Rough surfaces are generally more superhydrophobic due to their increased surface area. When a drop of water comes into contact with a rough surface, it interacts with more surface points compared to a smooth surface. This increased interaction results in a larger contact angle, which is a measure of hydrophobicity. In other words, on a rough surface, water droplets tend to aggregate and form spherical shapes to reduce their contact with the surface, resulting in a larger contact angle and thus increased hydrophobicity. This phenomenon is particularly evident on highly superhydrophobic surfaces, where the contact angle exceeds 150°. These results are consistent with the results of AFM studies, which showed that the surface roughness increases with increasing value of X value .

Table 3: Contact angle values of sponges coated with different x values

Sample	CA_L [°]	CA_R [°]	CA_AV [°]
x=0.05	150.3	151.5	151.5
x=0.2	158.8	158.9	158.8

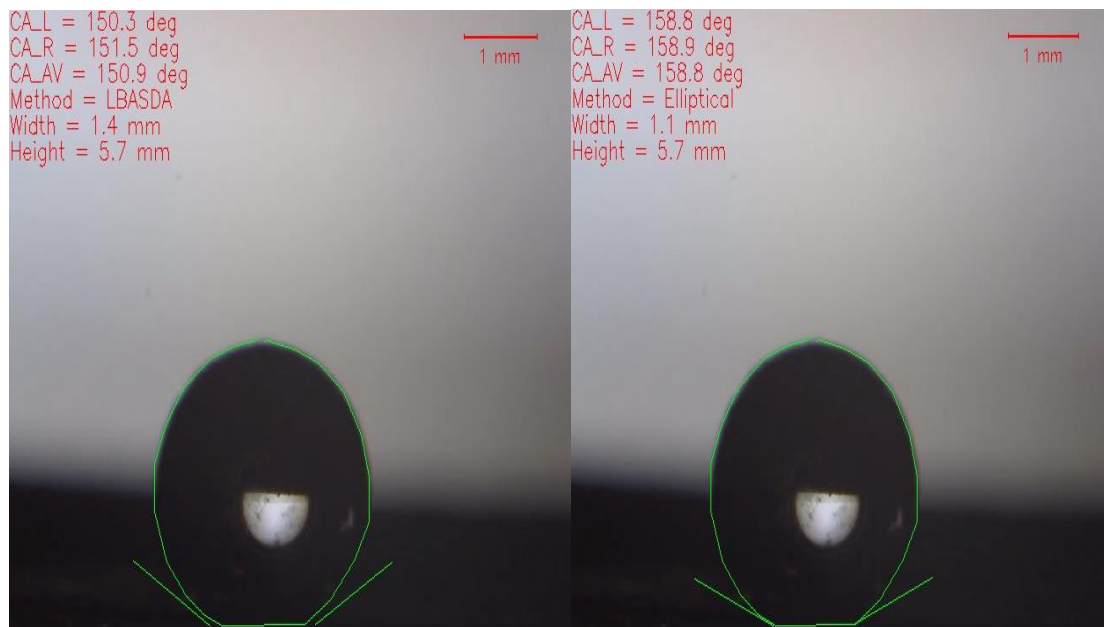


Figure 6. Contact angle measurements of coated sponges with different x values: (a) x=0.05 (b) x=0.2

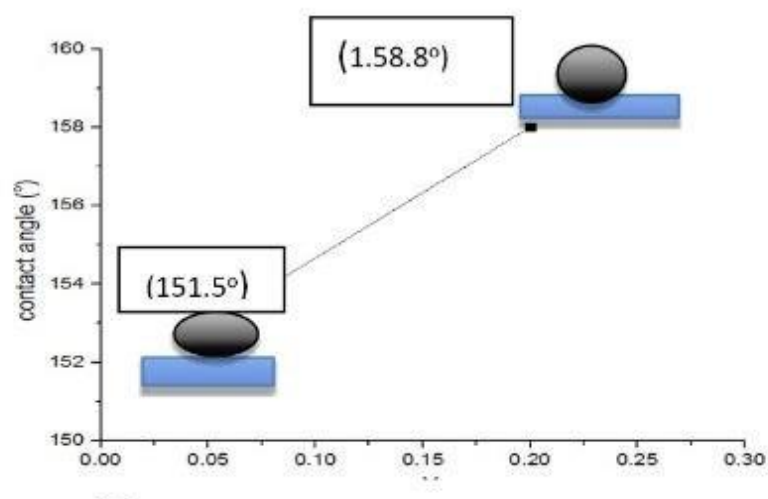


Fig. 7. Variation of contact angles for the coated sponges with different x values

4. Conclusions

In this research, sponges coated with a mixture of stearic acid, iron oxide, and magnesium oxide nanocomposites were successfully synthesized and characterized using different techniques such as XRD, FESEM, AFM, and Contact Angle measurements. XRD results showed the presence of iron oxide and magnesium oxide structures in the nanocomposites. FESEM studies revealed that all coated sponges showed a similar morphology and multilayer structure, with uniformly stacked nanocomposite sheets, providing complete coverage. The iron and magnesium oxide nanocomposites completely covered the network and porous structure and roughened the surface morphology of the sponge, as demonstrated by the SEM images. AFM analysis showed that the surface roughness of the coated sponge increased as the molar ratio of fatty acid to nanocomposite increased. The results of contact angle measurements showed that the wetting behavior of a liquid on a solid surface can be manipulated by changing the molar ratio of a fatty acid to a nanocomposite of iron oxide and magnesium oxide. As the molar ratio increased, the contact angle also increased, indicating enhanced superhydrophobicity.

References:

1. An, X., Chen, Y., Ao, M., Jin, Y., Zhan, L., Yu, B., ... & Jiang, P (2022). Sequential photocatalytic degradation of organophosphorus pesticides and recovery of orthophosphate by biochar/ α -Fe₂O₃/MgO composite: A new enhanced strategy for reducing the impacts of organophosphorus from wastewater. *Chemical Engineering Journal* 435, 135087.
2. Yavaş, A., Güneş, F., Erol, M., Sütçü, M., Güler, S., Kayalar, M. T., & Keskin, Ö. Y (2022). Development of visible light active self-cleaning clay roofing tiles as novel building materials: An investigation on the effects of α -Fe₂O₃ coating and firing temperature. *Journal of Cleaner Production* 362, 132302.
3. Ahuja, D., Dhiman, S., Rattan, G., Monga, S., Singhal, S., & Kaushik, A (2021). Superhydrophobic modification of cellulose sponge fabricated from discarded jute bags for oil water separation. *Journal of Environmental Chemical Engineering* 9(2), 105063.
4. Oliveira, S., Stojanovic, A., & Seeger, S. (2015). Superhydrophilic and superamphiphilic coatings. *Functional Polymer Coatings: Principles, Methods and Applications* 96-132.
5. Lu, J., Zhu, X., Miao, X., Wang, B., Song, Y., Ren, G., & Li, X (2020). An unusual superhydrophilic/superoleophobic sponge for oil-water separation. *Frontiers of Materials Science* 14, 341-350.

6. Yavaş, A., Güneş, F., Erol, M., Sütçü, M., Güler, S., Kayalar, M. T., & Keskin, Ö. Y. (2022). Development of visible light active self-cleaning clay roofing tiles as novel building materials: An investigation on the effects of α -Fe₂O₃ coating and firing temperature. *Journal of Cleaner Production* 362, 132302.
7. Rai, P. K., & Gupta, A. (2023). Development of durable anticorrosion superhydrophobic electroformed copper tubular structures. *Journal of Manufacturing Processes* 85, 236-245.
8. Abd Elkodous, M., El-Sayyad, G. S., Abdelrahman, I. Y., El-Bastawisy, H. S., Mosallam, F. M., Nasser, H. A., ... & El-Batal, A. I. (2019). Therapeutic and diagnostic potential of nanomaterials for enhanced biomedical applications. *Colloids and Surfaces B: Biointerfaces*, 180, 411-428.
9. Yavaş, A., Güneş, F., Erol, M., Sütçü, M., Güler, S., Kayalar, M. T., & Keskin, Ö. Y. (2022). Development of visible light active self-cleaning clay roofing tiles as novel building materials: An investigation on the effects of α -Fe₂O₃ coating and firing temperature. *Journal of Cleaner Production* 362, 132302.
10. Qayoom, M., Shah, K. A., Pandit, A. H., Firdous, A., & Dar, G. N. (2020). Dielectric and electrical studies on iron oxide (α -Fe₂O₃) nanoparticles synthesized by modified solution combustion reaction for microwave applications. *Journal of Electroceramics*, 45, 7-14.
11. Balakrishnan, G., Velavan, R., Batoor, K. M., & Raslan, E. H. (2020). Microstructure, optical and photocatalytic properties of MgO nanoparticles. *Results in Physics*, 16, 103013.